Synthesis and Stereochemical Properties of Chiral Square Complexes of Iron(II)

Thomas Bark,[a] Alexander von Zelewsky,*[a] Dmitrij Rappoport,[b] Markus Neuburger,[c] Silvia Schaffner,[c] Jérôme Lacour,[d] and Jonathan Jodry[d]

Abstract: The hexadentate, and ditopic ligand 2,5-bis([2,2′]bipyridin-6-yl)pyrazine yields a chiral, tetrameric, square-shaped, self-assembled species upon complexation with Fe^{2+} ions. The racemate of this complex was resolved with antimonyl tatrate as the chiral auxiliary. The purity of the enantiomer was determined by NMR spectroscopy, by using a chiral, diamagnetic shift reagent, and by circular dichroism (CD). The CD spectrum was also calculated by time-dependent density functional theory, and the correlation that was found between CD spectrum and configuration was confirmed by X-ray cristallography. When a "chiralised" version of the ligand was used instead, the corresponding iron complex was obtained in diastereomerically pure form.

Keywords: chiral resolution · density functional calculations · diastereoselectivity · iron · molecular squares · self-assembly

Introduction

On the vast playground of coordination-chemistry-based self-assembly reactions, one particularly prominent class of compounds are the so-called *molecular squares*. This term denotes a variety of complexes that have in common an arrangement of four metal ions or metal fragments in the corners of a square, connected through organic ligand strands. The ligands may coordinate through one donor atom, as for example, in the platinum- or palladium-based complexes developed by Fujita.[1,2] If the ligands coordinate by two or three donor atoms to each metal, chiral centres are created (As chirality descriptors, we use the "Oriented Line Reference System"[3,4]). Even if the metals represent centres of chirality, the entire complex can be achiral, if the arrangement of ligand strands is gridlike (type **A**, Figure 1). Examples are the complexes from tetrahedrally coordinated metal centres presented by the Osborn group,[5] as well as the related grids from the laboratories of Lehn,[6] and others[7–11] (for the exception of a chiral complex of type **A**, see Bassani et al.[12]).

If the four ligand strands "wrap" the four metal ions in an interwoven fashion, the resulting *molecular square* is a chiral complex (type **C**, Figure 1). The group of Dunbar

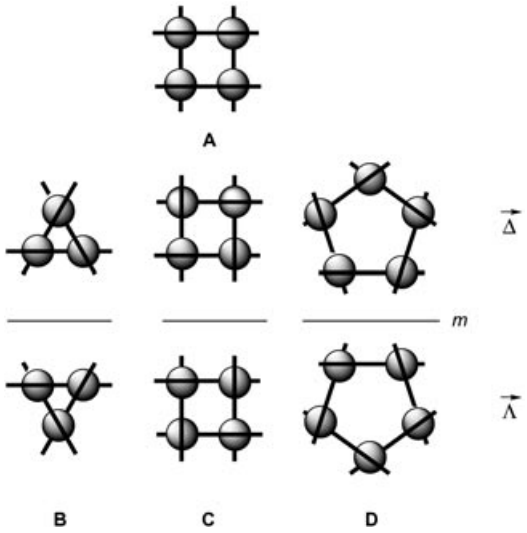

Figure 1. Schematic representation of several types of supramolecular complexes. The members of the second group (**B**, **C** and **D**) are chiral.

[a] T. Bark, Prof. A. von Zelewsky
Department of Chemistry
University of Fribourg, Pérolles
1700 Fribourg (Switzerland)
Fax: (+41) 26-300-9738
E-mail: alexander.vonzelewsky@unifr.ch

[b] D. Rappoport
Institute of Physical Chemistry
University of Karlsruhe, Kaiserstrasse 12
76128 Karlsruhe (Germany)

[c] M. Neuburger, S. Schaffner
Laboratory for Chemical Crystallography
University of Basel, Spitalstrasse 51
4056 Basel (Switzerland)

[d] J. Lacour, J. Jodry
Department of Organic Chemistry
University of Geneva, Quai Ernest Ansermet 30
1211 Genève (Switzerland)

 DOI: 10.1002/chem.200400399

published the first example, a nickel complex with the bis-bidentate ligand, 3,6-di-2-pyridyl-1,2,4,6-tetrazine.[13] Bu and co-workers followed with the corresponding zinc compound, which resolves spontaneously into single enantiomers upon crystallisation.[14] However, it was not possible for them to obtain larger amounts of enantiomerically pure complex in order to investigate its stereochemical properties. This might be due to the kinetic instability of the zinc complex. The tetrazine ligand does not occupy all coordination sites of the metal ions: in both cases, two solvent molecules per metal ion are needed to complete the quasi-octahedral coordination sphere. Our group has designed ligands that provide two terdentate terpyridine-type binding domains, that is, 2,5-bis([2,2′]bipyridin-6-yl)pyrazine (**L1**) and chiral derivatives of it.[15] These ligands were shown to yield tetrameric com-

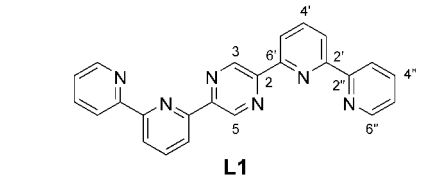

L1

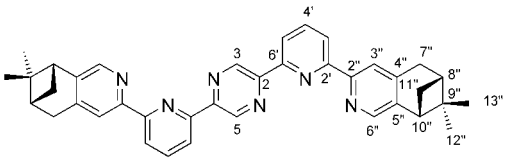

L2

plexes with zinc(II); no anchillary ligands are found in these complexes.[16] Whereas the complex $[Zn_4(\mathbf{L1})_4](PF_6)_8$ was obtained as racemic compound, "chiralised" ligand **L2** showed high diastereoselectivity and yielded $[Zn_4(\mathbf{L2})_4](PF_6)_8$ with 90% *de*. (The use of terpene-derivatised ligands for the predetermination of the configuration of chiral metal centres is a well-established method.[17]) These ligands that yield chiral, interwoven tetramers are also interesting for the fact that they are, in principle, not limited to the formation of tetramers. Unlike the pyrimidine-based ligands found in grid-type complexes[18] (**A**), they can also form complexes with an odd number of metal centres, for example, three (**B**) or five (**D**) (Figure 1). For example, Stoeckli-Evans published the solid structure of a trimer of type **B**.[19] Our group reported, that dissolved $[Zn_4(\mathbf{L1})_4](PF_6)_8$ is in equilibrium with its trimeric form $[Zn_3(\mathbf{L1})_3](PF_6)_6$,[16] and Dunbar et al. showed that it is possible to convert a nickel-based square into a pentagon by using a larger anion, which plays the role of a template.[20]

Abstract in German: *Der hexadentate und ditopische Ligand 2,5-Bis([2,2′]bipyridin-6-yl)pyrazin bildet bei der Selbstorganisationsreaktion mit Fe^{2+}-Ionen einen chiralen, quadratförmigen Tetramerkomplex. Das Racemat dieses Komplexes wurde mit Hilfe von Antimonyltartrat in die Enantiomere getrennt. Die Reinheit des Enantiomers wurde durch NMR-Spektroskopie unter Zuhilfenahme eines chiralen, diamagnetischen Shift-Reagenzes untersucht, wie auch duch die Beobachtung des Circulardichroismus (CD). Das CD-Spektrum wurde zudem mit zeitabhängiger Dichtefunktionaltheorie berechnet, wobei die vorhergesagte Korrelation zwischen CD-Spektrum und Konfiguration des Komplexes durch Röntgenstrukturanalyse bestätigt wurde. Die Verwendung einer "chiralisierten" Variante des Liganden ergab den entsprechenden Eisenkomplex in diastereomerenreiner Form.*

Discussion of Results

Complex synthesis: Although the related zinc complexes that we reported recently formed spontaneously upon combination of a zinc source, such as the perchlorate or fluoroborate, with the ligands (**L1** or **L2**) in the aprotic coordinating solvent MeCN, the corresponding iron(II) complexes could not be obtained in this way. Particularly **L1** yielded insoluble coordination polymers when treated with ferrous salts. We suspected these polymers to be kinetic intermediates, but even prolonged heating of this insoluble material in PhCN at reflux temperature failed to convert them into the discrete, tetrameric complex. Therefore, it was surprising to discover that the squares can be readily synthesised applying microwave heating: stoichiometric amounts of $[Fe(H_2O)_6](BF_4)_2$ and **L1** were heated in 9:1 ethylene glycol/water mixture for four minutes to reflux to furnish the desired complex $[Fe_4(\mathbf{L1})_4](PF_6)_8$ in quasi-quantitative yield after precipitation as hexafluorophosphate.

The dark green compound is diamagnetic and kinetically stable. Its NMR spectrum displays only eight signals, that is, half of all 16 ligand protons. This fact underlines the D_4 symmetry of the complex, whereby two of the four lateral C_2 axes divide each ligand into two equivalent halves. A detailed analysis of the shifts that proton resonances of the ligand undergo upon complexation confirms the circular structure of the complex (Figure 2): the protons H3 and H6″

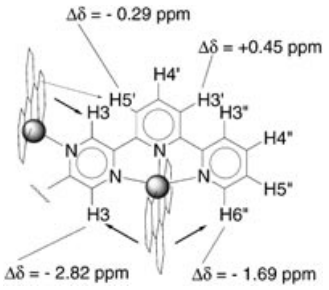

Figure 2. A fragment of the complex cation $[Fe_4(\mathbf{L1})_4]^{8+}$: Change in ^1H NMR shifts of the ligand **L1** upon complexation to Fe^{2+} are indicated.

are subject to considerable up-field shifts of $\Delta\delta = -2.82$ and -1.69 ppm, respectively. These shifts are due to the exposure of these protons to the magnet field provoked by the ring current of adjacent ligand molecules. The ring-shaped architecture of the complex becomes more evident when regarding the *m*-protons of the inner pyridine ring, H3′ and

H5′. These protons are chemically very similar and are hardly distinguished in the NMR spectrum of the free ligand. However, they behave differently within the complex: H5′ appears at higher field ($\Delta\delta = -0.29$ ppm), as it points towards a neighbouring ligand fragment. On the other hand, H3′, which points outside the complex, is shifted downfield ($\Delta\delta = +0.45$ ppm), as expected, due to the decrease of electron density in the complexed ligand.

The *nuclearity* of this circular assembly cannot be elucidated directly from the NMR spectrum, but electrospray ionisation mass spectrometry (ESI-MS) gave an answer to this question: (Figure 3) Only tetrameric fragments of the

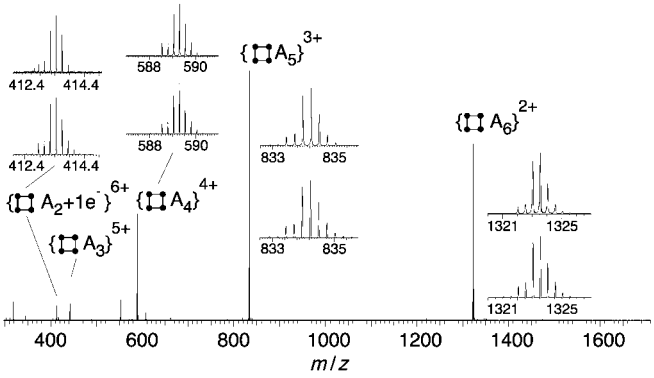

Figure 3. ESI mass spectrum of $[Fe_4(\mathbf{L1})_4](PF_6)_8$. The continuous loss of PF_6^- ions leads to series of fragments. Insets: Found (top) and calculated (bottom) isotopic distribution patterns.

type $\{[Fe_4(\mathbf{L1})_4](PF_6)_n\}^{8-n}$ with $n = 2$–6 are found in MeCN. Neither ESI-MS, nor NMR spectroscopy indicated the presence of a second, trimeric species; such a trimer was found to be a minor equilibrium product of the corresponding zinc(II) complex.

Resolution of the complex and stereochemical properties: As we have already stated in the introduction, complexes of the type of $[Fe_4(\mathbf{L1})_4](PF_6)_8$ are chiral, due to the interwoven arrangement of the ligand strands. All iron(II) ions are chiral-at-metal and have the same configuration within one complex cation. The entire complex ion can also be regarded as a short, quadruple-stranded helix. This helix is of *P* helicity, if the configuration of the metal ions is $\overrightarrow{\Lambda}$.

The complex is obtained as a racemate, evidently. It was separated by preferential crystallisation of diastereomeric salts, by using enantiomerically pure "antimonyl tartrate" (2*R*,2′*R*,3*R*,3′*R*)-$[Sb_2(tart)_2]^{2-}$ as the resolving agent. As the hexafluorophosphate salt of the complex is not soluble in water, the complex was transformed into the readily soluble chloride by simple metathesis reaction of $[Fe_4(\mathbf{L1})_4](PF_6)_8$ with NBu_4Cl in nitromethane, as $[Fe_4(\mathbf{L1})_4]Cl_8$ is insoluble in this solvent. Therefore it precipitates and can be isolated by filtration. (It is worth noting that this product could not be obtained by the reaction of $FeCl_2$ with **L1**.) The chloride was then dissolved in water and potassium antimonyl tartrate was added. In cases when the resolution was successful, one obtains brick-shaped crystals of up to 1 mm size. Unfortunately, this crystallisation process is very delicate, and in most cases we obtained an amorphous powder that contained both enantiomers of the complex cation. If seeding crystals are available from one successful run, the crystallisation becomes straightforward. X-ray crystallography revealed the chemical composition of the crystalline material to be $(\overrightarrow{\Lambda},\overrightarrow{\Lambda},\overrightarrow{\Lambda},\overrightarrow{\Lambda})$-$[Fe_4(\mathbf{L1})_4]Cl_2[Sb_2(tart)_2]_3$; the details of the structure will be discussed in the following paragraph. These crystals were then dissolved in water and the complex was again precipitated as the hexafluorophosphate salt. The resolved complex was investigated by UV-visible, CD and NMR spectroscopy. The optical absorption spectra shows two bands at 283 and 386 nm, which are due to ligand-centred transitions, as well as a strong MLCT band at around 680 nm ($\varepsilon = 6.98 \cdot 10^3\,l\,mol^{-1}\,cm^{-1}$ per Fe^{2+}). All these bands show strong CD activities (Figure 4). The most prominent

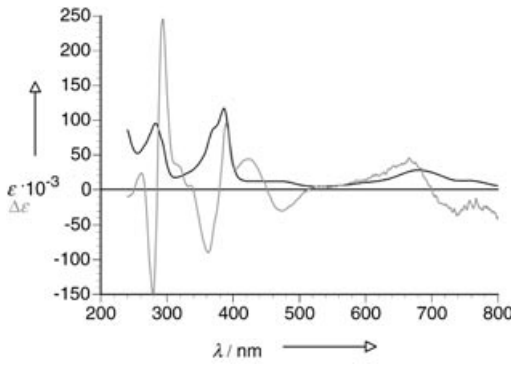

Figure 4. Optical properties of $(\overrightarrow{\Lambda})$-$[Fe_4(\mathbf{L1})_4](PF_6)_8$. Black: UV-visible spectrum; grey: CD spectrum.

effect is the exciton coupling of the 283 nm transition, which has a positive sign (i.e., the Cotton effect (CE) at longer wavelengths is positive, whereas the shortwave CE is negative and also has a smaller amplitude than the longwave CE). From these results we could not directly deduce the configuration of the complex: In contrast to the $[M(bpy)_3]^{n+}$ case, for which experimental and theoretical investigations of the CD activity are numerous in the literature,[21] we did not find any reports about the correlation of $[M(terpy^*)_2]^{n+}$ type complexes and their CD spectra (terpy* = an asymmetrical 2,2′:6′,2″-terpyridine). Thus the necessity of an X-ray analysis and the computational simulation of the CD-spectrum arose.

We also investigated the influence of the chiral, diamagnetic, anionic shift reagent Δ-TRISPHAT[22,23] on both the racemic and resolved complex. TRISPHAT (4.4 mol per mol of complex cation) was added to the complex, which was dissolved in $[D_3]$MeCN. Although signals for the two enantiomers of the complex cation are only poorly separated, as the induced shifts are relatively small (smaller than the line splitting of the signals), the enantiomeric purity of the resolved complex becomes evident (Figure 5).

The resolved complex is kinetically very stable. In dilute MeCN, we observed a decrease of CD activity only at elevated temperature (60 °C) over the course of several weeks.

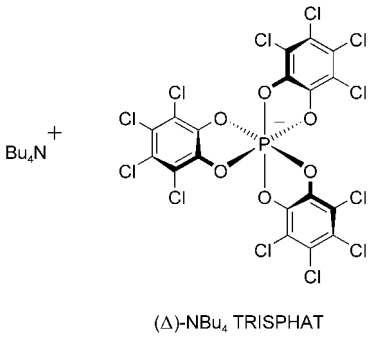

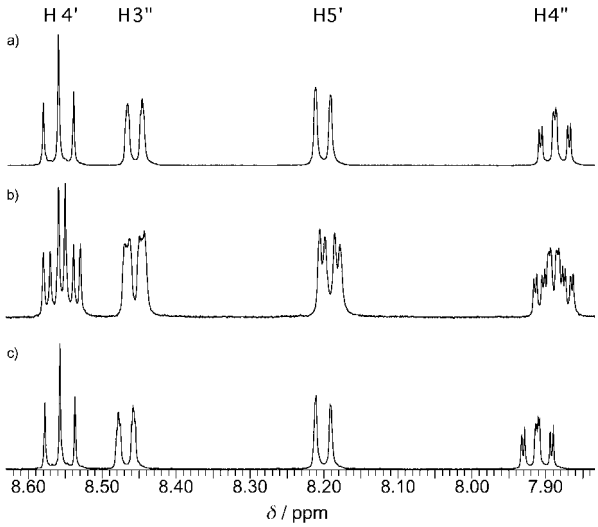

Figure 5. A part of the ^{1}H NMR spectrum of $[Fe_4(\mathbf{L1})_4](PF_6)_8$ in $[D_3]$MeCN. a) The racemic complex without additive, b) the racemic complex with Δ-TRISPHAT, c) the resolved complex with Δ-TRISPHAT.

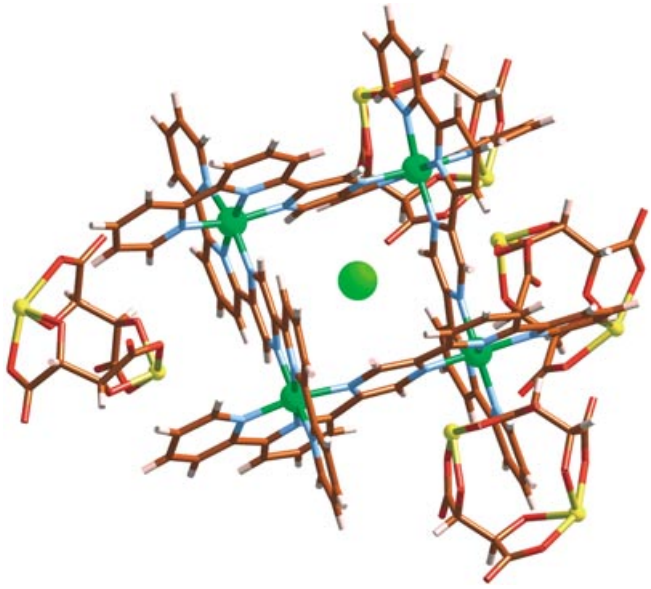

Figure 6. Top-view of the complex cation, alltogether with four antimonyl tartrate double helices. C: brown, N: blue, O: red, Cl: green, Fe: mint, Sb: yellow.

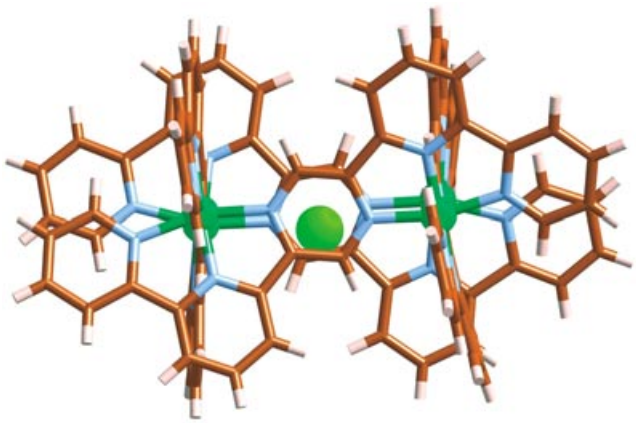

Figure 7. Side view of the complex cation, stressing the confinement of on chloride anion.

This decay is irregular and does not follow first-order reaction kinetics, as would be expected for a simple racemisation. Deterioration of the UV-visible spectrum and MS indicated that decomposition took place and $[Fe(\mathbf{L1})_2]^{2+}$ was mainly formed.

Crystal structure of $[Fe_4L1_4]Cl_2[Sb_2(tart)_2]_3$: As mentioned above, crystals of the antimonyl tartrate were submitted to an X-ray crystal structure analysis to confirm the structure of the complex and, more importantly, to establish the configuration of the crystallised enantiomer of the complex cation. The compound crystallises in the noncentrosymmetric space group $P2_1$. The asymmetric unit contains an entire $[Fe_4(\mathbf{L1})_4]^{8+}$ ion, three dimeric antimonyltartrate complex anions[24,25] and two chloride ions. One of the chloride ions occupies a position in the centre of the molecular square (Figures 6 and 7). Per complex cation, we find at least 54(!) water molecules; the exact number of which could not be determined by crystallography, due to the size and extreme water content of the compound. The water molecules and the antimonyl tartrate anions form an infinite network through hydrogen bonds (not shown). The complex cation displays the expected interwoven arrangement of ligand strands. The coordination environments of the four crystallographically independent iron(II) ions are in the expected range. The coordination geometry is a slightly distorted octahedron. The bond lengths for the sixteen metal-to-ligand bonds that lie within the plane of the square vary between 193 and 198 pm, wheras the remaining eight axial bonds are shorter; they range from 186 to 189 pm. This might be compared to simple $[Fe(terpy)_2]^{2+}$, for which a compression of the axial Fe–N-bonds has also been reported.[26] The configuration of the metal ions could be determined by correlation[27] to the stereocentres of the antimonyl tartrate anions (2*R*,2′*R*,3*R*,3′*R*)-$[Sb_2(tart)_2]^{2-}$ and it was found to be $\overrightarrow{\Lambda}$. This attribution was confirmed by the determination of the absolute structure of the crystal; the Flack parameter[28] for the structure containing the $\overrightarrow{\Lambda}$ complex cation and (*R*,*R*)-tartrate converged to $x = -0.01(1)$.

Diastereoselective complex formation: An alternative strategy towards stereochemically pure metal complexes, other

than racemate resolution, lies in the transfer of chirality from a chiral ligand to the metal centre. We applied this diastereoselective approach on the synthesis of such iron square complexes. Ligand **L2** is a "chiralised" version of **L1** (vide supra) bearing pinene fragments on the lateral pyridine rings at the 4″- and 5″-positions.

This ligand was treated with $[Fe(H_2O)_6](BF_4)_2$ as described above in the microwave oven. The hexafluorophosphate salt of the new complex was characterised by ESI-MS (which indicated its tetranuclearity), optical (Figure 8) and

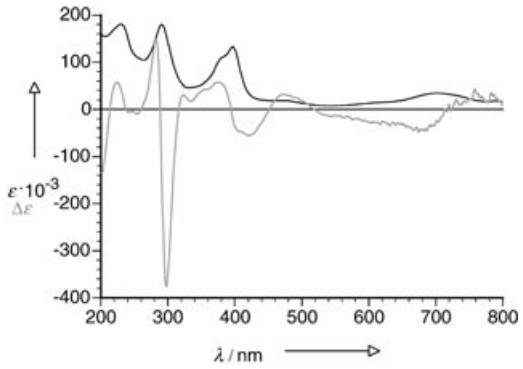

Figure 8. Optical properties of $(\overrightarrow{\Delta}_4)$-$[Fe_4(\mathbf{L2})_4](PF_6)_8$. Black: UV-visible spectrum, grey: CD spectrum.

NMR spectroscopy. The latter revealed the complete diastereoselectivity of the complexation reaction (within experimental errors); in the related zinc-case, a diastereomeric ratio (d.r.) of 95:5 was observed. The UV-visible spectrum of $[Fe_4(\mathbf{L2})_4](PF_6)_8$ is very similar to that of the complex with **L1**, but the mirrored CD spectrum indicates, that the configuration of the metal centres in $[Fe_4(\mathbf{L2})_4](PF_6)_8$ is $\overrightarrow{\Delta}$. This means that from the two possible diastereomers **E** and **F** (Figure 9), configuration **E** was chosen, in which the

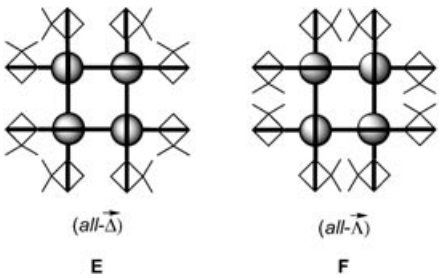

Figure 9. The two imaginable diastereomers of $[Fe_4(\mathbf{L2})_4](PF_6)_8$. **E** is the one actually formed.

methyl groups of the pinene moieties point to each other at the corners of the square, and not along the sides. This is the same situation as found in the major diastereomer of $[Zn_4(\mathbf{L2})_4](PF_6)_8$. It was not possible to grow X-ray-grade crystals of the iron(II)–**L2** complex.

Computational methods: To confirm experimental configuration assignment, TDDFT calculations for circular dichroism (CD) spectrum of $[Fe_4(\mathbf{L1})_4](PF_6)_8$ were performed. TDDFT has been recently shown to be well suited for calculation of CD spectra of simple transition-metal complexes[39] and is currently the only ab initio approach capable of treating systems of this size. A large number of electronic excitations of different origin are observed in the calculated spectrum, comprising more than 100 allowed transitions in the visible region. The high charge of $[Fe_4(\mathbf{L1})_4]^{8+}$ and the resulting strong interaction with counterions and solvent molecules, which is difficult to describe theoretically, is yet another source of error. Six inert PF_6^- ions were therefore included in the calculations to account for these interactions and to partly compensate the charge of the cation. The calculated CD spectrum of $\{[Fe_4(\mathbf{L1})_4](PF_6)_6\}^{2+}$ in the range up to 3 eV is shown in Figure 10 along with the experimental spec-

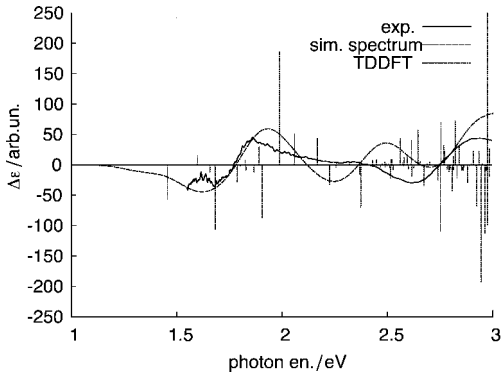

Figure 10. Found and calculated CD spectra of the enantiopure complex $[Fe_4(\mathbf{L1})_4](PF_6)_8$. For the calculated structure, the $\overrightarrow{\Lambda}$-configuration of the metal centres was assumed.

trum. A uniform line width of 0.1 eV was chosen to simulate line broadening. The TDDFT method is known to underestimate excitation energies by some tenth eV with the BP86 functional. Therefore, a blue-shift of 0.2 eV was applied to the calculated CD spectrum to account for these systematic errors and for the lacking solvation effects. Above 2.8 eV a very dense spectrum of electronic excitations appears in which cancellation of large rotatory strengths of opposite sign takes place. Some of these strong excitations arise from charge-transfer transitions from the PF_6^- ions and represent clearly artifacts of the calculation. For these reasons only the low-energy region <3 eV was used for configuration assignment in which these exciplex transitions have only little effect on the appearance of the CD spectrum. The strongest electronic excitations of this region are collected in Table 1. The CD spectrum is dominated by charge-transfer excitations from metal d orbitals into π^* orbitals of the ligands (MLCT), though an admixture of d→d transitions and ligand-metal charge transfer (LMCT) should be noted. Experimental and simulated spectra show semi-quantitative agreement in the considered range. In particular, the general pattern and the sign changes are correctly predicted, allowing for assignment of experimental CD spectrum to the $\overrightarrow{\Lambda}$ isomer of $[Fe_4(\mathbf{L1})_4](PF_6)_8$.

Table 1. Electronic excitations of $[Fe_4(\mathbf{L1})_4](PF_6)_8$ below 3 eV with rotatory strengths $>0.5\times10^{-38}$ erg cm^3.

Excitation	Exc. energy [eV]	Rot. strength [10^{-38} erg cm^3]	Interpretation
1^1A_2	1.36	−0.56	MLCT
3^1E	1.58	−1.05	MLCT
6^1A_2	1.81	−0.87	MLCT, d→d
10^1E	1.88	1.88	d→d
11^1E	1.96	0.52	π→π*, MLCT
16^1E	2.27	−0.70	MLCT
33^1E	2.54	0.57	MLCT
21^1A_2	2.65	0.70	π→π*, LMCT
39^1E	2.65	−1.09	exciplex
26^1A_2	2.72	0.73	MLCT, LMCT
59^1E	2.82	−0.67	MLCT
60^1E	2.84	−1.94	exciplex
61^1E	2.86	−1.13	exciplex, MLCT
63^1E	2.87	−0.99	MLCT
35^1A_2	2.87	6.00	exciplex

Experimental Section

Generalities: For the microwave heating, we used a standard household microwave oven, which was modified[29] in a way that allowed us to attach a reflux condenser to the heated reaction flask. For this purpose, a 2 cm hole was drilled into the top of the oven and a brace furnace ($L=$ 10 cm, outer $\phi=20$ mm, inner $\phi=18$ mm) was attached. Measurements showed no leakage of electromagnetical radiation. The reaction flask in the inner of the oven was then connected by menas of a glass tube with two ground joints to the reflux condenser on the outside. NMR spectra were recorded on Bruker Varian 400 and 500 spectrometers. UV-visible and CD spectra were measured on Perkin–Elmer Lambda 25 and Jasco J715 spectrometers, respectively. FT-ESI-MS measurements were performed on a Bruker BioAPEX II apparatus. $Fe(BF_4)_2{\cdot}x\,H_2O$ was purchased from Aldrich. To determine the actual iron content, an aliquot of it was reduced with Zn powder and HCl, before it was titrated with $KMnO_4$. The syntheses of **L1** and **L2** have been described elsewhere.[15]

Synthesis of (*rac*)-$[Fe_4(\mathbf{L1})_4](PF_6)_8$: $Fe(BF_4)_2{\cdot}x\,H_2O$ (280.9 μmol) was placed in a 250 mL flask and was dissolved in an ethylene glycol/water 9:1 mixture (3 mL). Ligand **L1** (109.1 mg, 208.9 μmol) and ascorbic acid (10 mg) were added. The mixture was heated to reflux under argon in a modified microwave oven for 4 min. The mixture turned dark green. The cooled mixture was diluted with MeCN (3 mL) and the complex was precipitated with aqueous NH_4PF_6 (1%, 100 mL). The complex was filtered off over Celite. It was washed with water and diethyl ether and was air-dried. The compound was redissolved in MeCN and purified by chromatography on a short column (silica 32–64 μm, MeCN +1% sat. aq. NH_4PF_6). The complex was isolated from the eluted fraction by precipitation, as described above. Yield: 208.5 mg (>99%), black powder. ^{1}H NMR (500.13 MHz, [D$_3$]MeCN): $\delta=8.96$ (dd, $J=8.3$, 0.8 Hz, 2H; H3′), 8.56 (dd, $J=8.3$, 8.1 Hz, 2H; H4′), 8.47 (dm, $J=8.1$ Hz, 2H; H3″), 8.21 (dd, $J=8.1$, 0.6 Hz, 2H; H5′), 7.91 (ddd, $J=8.2$, 8.1, 1.6 Hz, 2H; H4″), 7.06 (s, 2H; H3, H5), 7.02 (ddd, $J=5.7$, 1.5, 0.7 Hz, 2H; H6″), 6.98 ppm (td, $J=5.7$, 1.3 Hz, 2H; H5″); NOE Diff.: 8.96 (8.56, +1.9%; 8.47, +2.7%); 8.47 (8.96, +2.6%, 7.91, +2.2%); 8.21 (8.56, +2.0%; 7.06, +3.9%); ^{13}C NMR (125.76 MHz, [D$_3$]MeCN): $\delta=160.21$ (q), 157.54 (q), 156.84 (q), 155.85 (q), 154.14 (C6″), 146.20 (C3), 140.92 (C4″), 139.31 (C4′), 128.76 (C5″), 128.18 (C5′), 126.65 (C3′), 125.85 ppm (C3″); ESI-MS (MeCN): m/z (%): 1326 (72) $\{[Fe_4(\mathbf{L1})_4](PF_6)_6\}^{2+}$, 834 (100) $\{[Fe_4(\mathbf{L1})_4](PF_6)_5\}^{3+}$, 589 (43) $\{[Fe_4(\mathbf{L1})_4](PF_6)_4\}^{4+}$, 442 (13) $\{[Fe_4(\mathbf{L1})_4](PF_6)_3\}^{5+}$, 413 (6) $\{[Fe_4(\mathbf{L1})_4](PF_6)_2+1e^-\}^{5+}$; high-resolution ESI-MS (MeCN): $\{[Fe_4(\mathbf{L1})_4](PF_6)_5\}^{3+}$, $C_{96}H_{64}{}^{56}Fe_4F_{30}N_{24}P_5$ requires m/z: 833.7115210; found: 833.7112016; error: $3.194\cdot10^{-4}$.

Resolution of (*rac*)-$[Fe_4(\mathbf{L1})_4](PF_6)_8$: The complex (52.8 mg, 18.0 μmol) was dissolved in $MeNO_2$ (4 mL) and a solution of NBu_4Cl (400 mg, 1.44 mmol) in $MeNO_2$ (4 mL) was added. $[Fe_4(\mathbf{L1})_4]Cl_8$ precipitated and was isolated by centrifugation. The product was washed several times with EtOAc, then with diethyl ether. A solution of "K[Sb(tartrate)]·$3\,H_2O$" (16.1 mg, 52 μmol) in water (0.8 mL) was added to a filtered solution of this chloride salt in water (0.8 mL). If available, some seeding crystals were added. The mixture was kept at room temperature for 24 h, followed by another 24 h at 4°C. The resolved complex crystallised in dark, brick-shaped crystals (if an amorphous powder was obtained instead, the resolution procedure had failed). The mother liquor was removed and the crystals were washed with a little cold water. They were then dissolved in water (30 mL) and NH_4PF_6 (300 mg) was added. The precipitated hexafluorophosphate salt was filtered off over Celite. It was washed with water and diethyl ether and was air-dried. Yield: 14.6 mg (55%); UV/Vis (MeCN): λ_{max} (ε) = 283 (9.53×10^4), 368 sh (8.42×10^4), 386 (1.17×10^5), 682 nm (2.79×10^4 mol^{-1}dm^{3}cm^{-1}); CD (MeCN): $\lambda_{min/max}$ ($\Delta\varepsilon$) = 261 (23.4), 279 (−150), 293 (254), 362 (−89.9), 386 (117), 422 (43.9), 474 (−29.7), 665 (45), 737 nm (−36 mol^{-1}dm^{3}cm^{-1}).

Crystallographic analysis of $[Fe_4\mathbf{L1}_4]Cl_2[Sb_2(tart)_2]_3$: Formula: $C_{120}H_{76}Cl_2Fe_4N_{24}O_{36}Sb_6{\cdot}54\,H_2O$, $M_r=4427.61$; dark green plate, crystallised from water, $0.32{\cdot}0.32{\cdot}0.14$ mm^3, monoclinic, space group $P2_1$, $Z=2$, $a=16.3525(5)$, $b=32.9157(8)$, $c=18.1155(5)$ Å, $\alpha=\gamma=90°$, $\beta=105.625°$, $V=9390.4$ Å^3. $\rho_{calcd}=1566$ kg m^{-3}. The crystal was measured on a Bruker–Nonius KappaCCD area detector, at 173 K, using graphite-monochromated $Mo_{K\alpha}$ radiation with $\lambda=0.71073$ Å, $2\theta_{max}=57.0°$; min/max transmission 0.66/0.84, $\mu=1.275$ mm^{-1}. From a total of 148457 reflections, 46022 were independent. From these, 35471 were considered as observed [$I>3\sigma(I)$] and were used to refine 2367 parameters. The structure was solved by direct methods. Least-squares refinement against $|F|$ was carried out on all non-hydrogen atoms. $R=0.0486$ (observed data), $wR=0.0516$ (all data), GOF = 1.019. Min/max residual electron density = −3.56/3.55 e Å^{-3}. The Flack-parameter for the chosen absolute structure was $x=0.01(1)$.

60 positions of water-based oxygen atoms were localised; 33 of which were considered as normally occupied, 8 as disordered and 19 as partially occupied. As the electron density of the remaining maxima of the difference Fourier map decrease continuously, the actual number of water molecules could not be determined precisely. The water protons could not be located. CCDC-208876 contains the supplementary crystallographic data for this paper. These data can be obtained free of charge via www.ccdc.cam.ac.uk/conts/retrieving.html (or from the Cambridge Crystallographic Data Centre, 12 Union Road, Cambridge CB21EZ, UK; fax: (+44) 1223-336-033; or deposit@ccdc.cam.ac).

Synthesis of $(\vec{\Delta},\vec{\Delta},\vec{\Delta},\vec{\Delta})$-$[Fe_4(\mathbf{L2})_4](PF_6)_8$: $Fe(BF_4)_2{\cdot}x\,H_2O$ (93.3 μmol) and **L2** (53.8 mg, 93.3 μmol) were reacted together by using a similar procedure to that described for (*rac*)-$[Fe_4(\mathbf{L1})_4](PF_6)_8$. Diasteriomerically pure $(\vec{\Delta},\vec{\Delta},\vec{\Delta},\vec{\Delta})$-$[Fe_4\mathbf{L2}_4](PF_6)_8$ (81.2 mg, 94%) was obtained after chromatography and precipitation. ^{1}H NMR (500.13 MHz, [D$_3$]MeCN): $\delta=$ 8.86 (dd, $J=8.3$, 0.8 Hz, 2H; H3′), 8.51 (t, $J=8.2$ Hz, 2H; H4′), 8.28 (s, 2H; H3, H5), 8.13 (dd, $J=8.2$, 0.8 Hz, 2H; H5′), 7.02 (s, 2H; H3″), 6.45 (s, 2H; H6″), 2.99 (m, 4H; $H_{pro\text{-}R}7''$, $H_{pro\text{-}S}7''$), 2.33 (dt, $J=9.9$, 5.8 Hz, 2H; $H_{pro\text{-}S}11$), 2.26 (t, $J=5.5$ Hz, 2H; H10″), 2.10 (ddd, $J=8.2$, 5.6, 2.6 Hz, 2H; H8″), 1.08 (s, 6H; H13″), 0.59 (d, $J=10.0$ Hz, 2H; $H_{pro\text{-}R}11''$), 0.02 ppm (s, 6H; H12″); ^{13}C NMR (125.76 MHz, [D$_3$]MeCN): $\delta=160.58$ (q), 156.25 (q), 155.85 (q), 155.19 (q), 150.76 (q), 149.21 (q), 148.36 (C6″), 145.65 (C3″), 139.09 (C4′), 127.30 (C5′), 125.86 (C3′), 125.26 (C3,C5), 44.70 (C10″), 39.88 (C8″), 38.98 (q, C9″), 33.41 (C7″), 30.50 (C11″), 25.25 (C13), 20.74 ppm (C12). ESI-MS (MeCN): m/z (%): 1700 (11) $\{[Fe_4(\mathbf{L2})_4](PF_6)_6\}^{2+}$, 1085 (27) $\{[Fe_4(\mathbf{L2})_4](PF_6)_5\}^{3+}$, 778 (76) $\{[Fe_4(\mathbf{L2})_4](PF_6)_4\}^{4+}$, 593 (100) $\{[Fe_4(\mathbf{L2})_4](PF_6)_3\}^{5+}$, 564 (12) $\{[Fe_4(\mathbf{L2})_4](PF_6)_2+e^-\}^{5+}$, 470 (95) $\{[Fe_4(\mathbf{L2})_4](PF_6)_2\}^{6+}$; high resolution ESI-MS (MeCN): $\{[Fe_4(\mathbf{L2})_4](PF_6)_5\}^{3+}$, $C_{152}H_{144}F_{30}{}^{56}Fe_4N_{24}P_5$ requires m/z: 1084.5865357; found: 1084.5865290; error: $6.7\cdot10^{-6}$; UV/Vis (MeCN): λ_{max} (ε) = 232 (1.80×10^5), 291 (1.80×10^5), 382 (1.10×10^5), 397 (1.33×10^5), 480 (1.79×10^4), 702 nm (3.42×10^4 mol^{-1}dm^{3}cm^{-1}); CD (MeCN): $\lambda_{min/max}$ (ε) = 224 (57), 254 (−10), 282 (148), 298 (−376), 323 (31), 334 (min 17), 375 (57), 421 (−55), 474 (32), 674 (-5×10^2), 758 nm (6×10^2 mol^{-1}dm^{3}cm^{-1}).

Computational details: All calculations were performed within the framework of density functional theory (DFT) employing gradient-corrected BP86 functional.[30,31] We used a split-valence basis set with polarisation functions on non-hydrogen atoms (SV(P)[32]) together with efficient RI-J approximation for Coulomb matrix elements.[33] The ground state geometry of $[Fe_4(\mathbf{L1})_4](PF_6)_8$ was fully optimised within D_4 symmetry. For the optimised structure, electronic excitation energies and corre-

sponding rotatory strengths were calculated with time-dependent density functional theory (TDDFT).[34–36] Interpretation of character of electronic transitions was based on the analysis of excitation vectors.[37] The Turbomole[38] programme suite was used for all calculations.

Acknowledgement

This work is financially supported by the Swiss National Science Foundation. We thank Mr. Ivan Schindelholz for the synthesis of ligand **L1** and Mr. Freddy Nydegger for recording MS spectra. D.R. thanks Prof. R. Ahlrichs and Dr. F. Furche for support and valuable discussions.

[1] M. Fujita, J. Yazaki, K. Ogura, *J. Am. Chem. Soc.* **1990**, *112*, 5645–5647.
[2] M. Fujita, J. Yazaki, K. Ogura, *Chem. Lett.* **1991**, 1031–1032.
[3] T. Damhus, C. E. Schäffer, *Inorg. Chem.* **1983**, *22*, 2406–2412.
[4] A. von Zelewsky, *Stereochemistry of Coordination Compounds*, Wiley, Chichester (UK), **1995**, p. 70.
[5] M. T. Youinou, N. Rahmouni, J. Fischer, J. A. Osborn, *Angew. Chem.* **1992**, *104*, 771–773; *Angew. Chem. Int. Ed. Engl.* **1992**, *31*, 733–735,
[6] M. Ruben, E. Breuning, M. Barboiu, J.-P. Gisselbrecht, J.-M. Lehn, *Chem. Eur. J.* **2003**, *9*, 291–299.
[7] J. R. Galan-Mascaros, K. R. Dunbar, *Chem. Commun.* **2001**, 217–218.
[8] H. Grove, J. Sletten, M. Julve, F. Lloret, J. Cano, *J. Chem. Soc. Dalton Trans.* **2001**, 259–265.
[9] N. D. Sung, K. S. Yun, T. Y. Kim, K. Y. Choi, M. Suh, J. G. Kim, I. H. Suh, J. Chin, *Inorg. Chem. Commun.* **2001**, *4*, 377–380.
[10] R. Krämer, L. Kovbasyuk, H. Pritzkow, *New J. Chem.* **2002**, *26*, 516–518.
[11] J. P. Plante, P. D. Jones, D. R. Powell, T. E. Glass, *Chem. Commun.* **2003**, 336–337.
[12] D. M. Bassani, J.-M. Lehn, K. Fromm, D. Fenske, *Angew. Chem.* **1998**, *110*, 2534–2537; *Angew. Chem Int. Ed.* **1998**, *37*, 2364–2367.
[13] C. S. Campos-Fernandez, R. Clerac, K. R. Dunbar, *Angew. Chem.* **1999**, *111*, 3685–3688; *Angew. Chem. Int. Ed.* **1999**, *38*, 3477–3479.
[14] X.-H. Bu, M. Hiromasa, K. Tanaka, K. Biradha, S. Furusho, M. Shionoya, *Chem. Commun.* **2000**, 971–972.
[15] T. Bark, H. Stoeckli-Evans, A. von Zelewsky, *J. Chem. Soc. Perkin Trans. 1* **2002**, 1881–1886.
[16] T. Bark, M. Düggeli, H. Stoeckli-Evans, A. Von Zelewsky, *Angew. Chem.* **2001**, *113*, 2924–2927; *Angew. Chem. Int. Ed.* **2001**, *40*, 2848–2851.
[17] A. von Zelewsky, O. Mamula, *J. Chem. Soc. Dalton Trans.* **2000**, 219–231.
[18] E. Breuning, G. S. Hanan, F. J. Romero-Salguero, A. M. Garcia, P. N. W. Baxter, J.-M. Lehn, E. Wegelius, K. Rissanen, H. Nierengarten, A. Van Dorsselaer, *Chem. Eur. J.* **2002**, *8*, 3458–3466.
[19] A. Neels, H. Stoeckli-Evans, *Inorg. Chem.* **1999**, *38*, 6164- 6170.
[20] C. S. Campos-Fernandez, R. Clerac, J. M. Koomen, D. H. Russell, K. R. Dunbar, *J. Am. Chem. Soc.* **2001**, *123*, 773–774.
[21] M. Ziegler, A. Von Zelewsky, *Coord. Chem. Rev.* **1998**, *177*, 257–300.
[22] J. Lacour, C. Ginglinger, C. Grivet, G. Bernardinelli, *Angew. Chem.* **1997**, *109*, 660–662; *Angew. Chem. Int. Ed.* **1997**, *36*, 608–609.
[23] J. Lacour, V. Hebbe-Viton, *Chem. Soc. Rev.* **2003**, *32*, 373–382, and references therein.
[24] H.-C. Mu, *Kexue Tongbao (Chin. Ed.)* **1966**, 17, 502–504 [*Chem. Abstr.* **1967**, 69731].
[25] M. E. Gress, R. A. Jacobson, *Inorg. Chim. Acta* **1974**, *8*, 209–217.
[26] A. T. Baker, H. A. Goodwin, *Aust. J. Chem.* **1985**, *38*, 207–214.
[27] A. Zalkin, D. H. Templeton, T. Ueki, *Inorg. Chem.* **1973**, *12*, 1641–1646.
[28] H. D. Flack, *Acta Crystallogr. Sect. A* **1983**, *39*, 876–881.
[29] E. Jandrasics, Ph.D. Thesis, No. 1085, University of Fribourg (Switzerland), Faculty of Science, **1995**.
[30] A. D. Becke, *Phys. Rev. A* **1988**, *38*, 3098–3100.
[31] J. P. Perdew, W. Yue, *Phys. Rev. B* **1986**, *33*, 8800–8802.
[32] A. Schäfer, H. Horn, R. Ahlrichs, *J. Chem. Phys.* **1992**, *97*, 2571–2571.
[33] K. Eichkorn, O. Treutler, H. Öhm, M. Häser, R. Ahlrichs, *Chem. Phys. Lett.* **1995**, *240*, 283–289.
[34] M. E. Casida in *Recent Advances in Density Functional Methods* (Ed.: D. P. Chong), World Scientific, Singapore, **1995**, p. 155.
[35] R. Bauernschmitt, R. Ahlrichs, *Chem. Phys. Lett.* **1996**, *256*, 454–464.
[36] R. Bauernschmitt, M. Häser, O. Treutler, R. Ahlrichs, *Chem. Phys. Lett.* **1997**, *264*, 573–578.
[37] F. Furche, R. Ahlrichs, C. Wachsmann, E. Weber, A. Sobanski, F. Vögtle, S. Grimme, *J. Am. Chem. Soc.* **2000**, *122*, 1717–1724.
[38] R. Ahlrichs, M. Bär, M. Häser, H. Horn, C. Kölmel, *Chem. Phys. Lett.* **1989**, *162*, 165–169, also see http://www.turbomole.de.
[39] J. Autschbach, F. E. Jorge, T. Ziegler, *Inorg. Chem.* **2003**, *42*, 2867–2877.

Received: April 23, 2004
Published online: August 17, 2004

